

# PCCP

Accepted Manuscript



This is an *Accepted Manuscript*, which has been through the Royal Society of Chemistry peer review process and has been accepted for publication.

*Accepted Manuscripts* are published online shortly after acceptance, before technical editing, formatting and proof reading. Using this free service, authors can make their results available to the community, in citable form, before we publish the edited article. We will replace this *Accepted Manuscript* with the edited and formatted *Advance Article* as soon as it is available.

You can find more information about *Accepted Manuscripts* in the [Information for Authors](#).

Please note that technical editing may introduce minor changes to the text and/or graphics, which may alter content. The journal's standard [Terms & Conditions](#) and the [Ethical guidelines](#) still apply. In no event shall the Royal Society of Chemistry be held responsible for any errors or omissions in this *Accepted Manuscript* or any consequences arising from the use of any information it contains.

Cite this: DOI: 10.1039/xxxxxxxxxx

## Tuning magnetic properties of antiferromagnetic chains with exchange interactions: *ab initio* studies

Kun Tao,<sup>\*ab c</sup> Qing Guo,<sup>a</sup> Puru Jena,<sup>b</sup> Desheng Xue<sup>a</sup> and V.S. Stepanyuk<sup>c</sup>Received Date  
Accepted Date

DOI: 10.1039/xxxxxxxxxx

www.rsc.org/journalname

The possibility of using exchange interactions to manipulate the spin state of an antiferromagnetic nanostructure is explored with *ab initio* calculations. Taking M (M = Mn, Fe, Co) mono-atomic chains supported on Cu<sub>2</sub>N islands on a Cu(001) surface as a model system, it is demonstrated that two indistinguishable Néel states of an antiferromagnetic chain can be tailored into a preferred state by the exchange interaction with a magnetic STM tip. The magnitude and direction of the anisotropy for antiferromagnetic chains can also be tuned with the exchange coupling by varying the tip-chain separation.

For a long time the attention of scientific and engineering communities engaged in the business of spintronics has been given almost exclusively to ferromagnetic systems because their spin orientation can be switched by magnetic fields or spin-torque currents.<sup>1</sup> At the atomic level or even at the subnanometer scale, the possibility to precisely manipulate spin states of a magnetic storage unit with magnetic field is a big problem since the inherent non-locality of the field may result in unwanted spin flips of neighboring units. Only recently “antiferromagnetic (AFM) spintronics”, which is insensitive to magnetic field due to a lack of net magnetic moment, has started to gain popularity<sup>2</sup> due to its great advantage for applications where stability against stray magnetic fields is crucial.<sup>3–5</sup> Artificial AFM nanostructures have been featured in a number of remarkable experiments, ranging from fundamental studies of elementary spin excitations to realization of all-spin-based logic gate.<sup>2,6–9</sup> However, the spin state of an AFM material is hard to control with external magnetic field due to its zero net spin. The question how to manipulate the spin state of an AFM material then becomes one of the major obstacles for its application in spintronics industry. Up to now, only a few potential solutions have been offered.<sup>2,10,11</sup>

The second major requirement for spintronic devices at the atomic level has always been the inherent thermal stability of their macro-spin. As the dimensions of a system shrink down to the size of a few hundred atoms, the system tends to start behaving super-paramagnetically. To stabilize the spin orientation against thermal fluctuations, a large magnetic anisotropy energy (MAE) is required. Many strategies to enhance the MAE of magnetic materials have been proposed, such as alloying,<sup>12–14</sup>

exposure to external electric field,<sup>15–20</sup> local environment manipulation,<sup>21,22</sup> electron or hole injection,<sup>23</sup> and the use of low-coordination anisotropic geometries.<sup>24–26</sup> However, nearly all of them focus on ferromagnetic materials, and very few works are on AFM systems.

In the present work we shall address a special class of low-dimensional antiferromagnetic structures – linear atomic chains, which can classically be found in one of the two Néel states  $|1\rangle = |\dots, \uparrow, \downarrow, \uparrow, \downarrow, \dots\rangle$  and  $|2\rangle = |\dots, \downarrow, \uparrow, \downarrow, \uparrow, \dots\rangle$ , where the arrows denote the spin orientation of a particular atom in the chain. It is, however, known from both theoretical and experimental studies, that atomic spins of AFM chains often behave as quantum objects<sup>27–29</sup>. Recent experiments confirmed the existence of a classical-to-quantum transition of an atomic chain’s behavior when the parity of the chain-length changes from odd to even<sup>30</sup>. It was reported in both experiment and theory that the quantum ground state of an AFM atomic chain can be tailored into one of the two Néel states by passing a tunneling current through the system via a scanning tunneling microscope (STM) tip<sup>2,10</sup>. Recently, it has been demonstrated that the exchange coupling with the STM tip can be used to tune the spin mixing of a finite AFM chain<sup>11</sup>.

Here, using *ab initio* tools and choosing M/Cu<sub>2</sub>N/Cu(001) (M = Mn, Fe, Co) as a model system, we demonstrate that exchange coupling with the magnetic STM tip can be used to tailor two degenerated ground states of an AFM system into different classical Néel states. We further demonstrate that both amplitude and sign of the magnetic anisotropy of the AFM system can be tuned by the exchange coupling.

### 1 Calculation methods

Our calculations were carried out in the framework of Density Functional Theory (DFT) as implemented in Vienna *Ab initio* Sim-

<sup>a</sup> Key Lab for Magnetism and Magnetic Materials of Ministry of Education, Lanzhou University, Lanzhou 730000, People’s Republic of China E-mail: taokun@lzu.edu.cn

<sup>b</sup> Physics Department, Virginia Commonwealth University, Richmond, VA, USA

<sup>c</sup> Max-Planck-Institute of Microstructure Physics, Halle, Germany

ulation Package (VASP)<sup>31,32</sup> with the projector augmented wave (PAW) potentials<sup>33</sup> and the generalized gradient approximation (GGA) due to Perdew, Burke and Ernzerhof (PBE)<sup>34</sup>. The basis set contained plane waves with a kinetic energy cutoff of 500 eV and the total energy was converged to  $10^{-7}$  eV. All geometries were optimized without any symmetry constraint until all residual forces on each atom were less than 0.01 eV/Å. Spin-orbit coupling (SOC) with relativistic effect was included in all calculations.

A  $3 \times 4$  supercell is employed in all calculations, and the distance between two neighbouring supercells is larger than 10 Å. The supercell consists of 5 Cu(001) layers with a  $c(2 \times 2)N$ -Cu(001) molecular network on one side, in which magnetic nanoscale systems are partially screened from the metallic support by a thin decoupling layer<sup>2,21,22,26,28</sup>. Magnetic adatoms are known to reside on top of Cu sites of  $Cu_2N^2$ . In our calculation, 4 magnetic atoms were placed to form a compact infinite chain which means the distance between two magnetic atoms is about 3.6 Å, as sketched in Fig. 1(a) and (b). Magnetic atoms on  $Cu_2N$  push the Cu atoms directly beneath them deeper into the Cu(001) substrate. The surrounding N atoms are, on the contrary, pulled outwards from the surface forming bonds with magnetic adsorbates. To mimic the influence of the STM tip on the magnetic properties of the chain on surface, we used 9 Cu atoms and 1 Cr atom as the apex of the tip. Such a tip can be obtained in experiment by attaching atoms to the tip apex<sup>11</sup> and we have used this model many times, for example in Ref. <sup>35</sup>. Relaxed geometry obtained in our calculations agrees well with experimental<sup>2,11,25</sup> and previous theoretical<sup>36-38</sup> results.

## 2 Results and discussion

The bonding between the neighboring magnetic atoms is mediated by N atoms of the surface molecular  $Cu_2N$  network residing between them, or in other words, the magnetic atoms interact with each other by the super-exchange interactions. We calculated the exchange interaction between magnetic atoms in the chain as  $J_{MM} = \Delta E / 4S_M^2 = (E_P - E_{AP}) / 4S_M^2$ .  $\Delta E$  is the energy difference between parallel ( $E_P$ ) and antiparallel ( $E_{AP}$ ) spin configurations for the chain, and  $S_M$  is the spin of the magnetic atom. We took a pure Fe chain (without STM tip) on  $Cu_2N$  surface as an example, according to our calculations, the spin of the Fe atom is around  $S=1.5$ , which was used for the following parts. The exchange interaction  $J_{MM}$  for a compact Fe chain increases from 18.7 meV per Fe pair on Cu(001) surface to 35.2 meV on  $Cu_2N$  surface. The exchange interaction  $J_{MM}$  in experiments for the Mn chain<sup>6</sup> and the Fe chain<sup>2,11</sup> on  $Cu_2N$  surface is about 6.2 meV and 1.2 meV respectively, which is much smaller than our results. This is due to that the distance between two Fe atoms in the compact chain being 3.6 Å while it is 7.2 Å for the Mn (Fe) chain in experiment. We also calculated the exchange interaction of a 3 Fe atoms composed finite chain on  $Cu_2N$  surface, in which the distance between two Fe atoms was 7.2 Å, similar to that in experiments.<sup>11</sup> The exchange interaction  $J_{MM}$  between Fe atoms is greatly reduced to about 2.7 meV. Therefore, the super-exchange interaction between magnetic atoms not only aligns the spins of the neighboring magnetic adatoms anti-parallel to each other, but also enhances interactions between them.

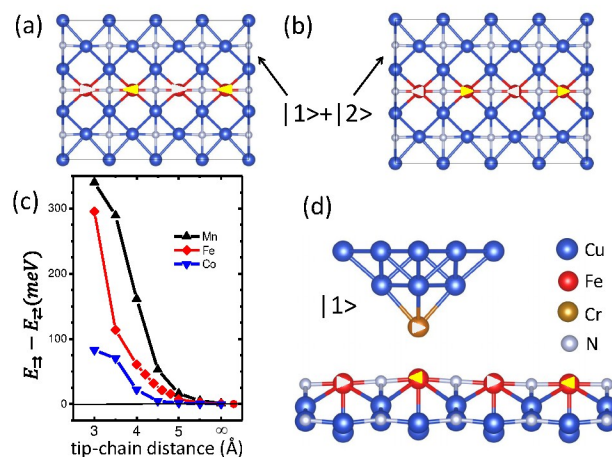


**Fig. 1** (a) and (b) schematically demonstrate magnetic chains on a  $Cu_2N/Cu(001)$  substrate in an correlated state of superposition of two Néel states  $|1\rangle$  and  $|2\rangle$ . (c) Dependence of the exchange coupling between a Cr-terminated STM tip and magnetic chains on substrate on the distance between the tip apex and the chain. The last point marked with “∞” underlines the absence of exchange in absence of a tip. (d) a collapsed state  $|1\rangle$  due to exchange coupling to the Cr tip placed over one of the magnetic atoms. Small triangles with different colors represent different spin directions.

As was mentioned before, in absence of external influence, the two Néel states of the chain ( $|1\rangle$  and  $|2\rangle$ ) have the same total energy and are quantum-mechanically indistinguishable. In a ferromagnet, the degeneracy of a spin state can usually be lifted by applying an external magnetic field. In an anti-ferromagnetic system, where the net spin of the system is zero, the Zeeman splitting cannot be relied on anymore, since it acts equally on both Néel states. One way to lift the degeneracy and tune the quantum AFM system into one of the classical states is by a dynamic perturbation, such as the tunneling current from an STM tip,<sup>2</sup> or the exchange interaction between the tip and the sample.<sup>11</sup> Here, we propose that the exchange interaction between the chain and the tip can act as a local perturbation and favor one of the Néel states over the other, thus lifting the degeneracy and tuning the AFM chain into one of its classical states<sup>§</sup>.

The magnitude of the exchange interaction  $E_{exch}$  between a Cr-terminated STM tip and a  $M/Cu_2N/Cu(001)$  ( $M = Mn, Fe, Co$ ) chain when the tip is positioned right above one of the magnetic atoms of the chain, is plotted in Fig. 1(c) as a function of the tip-chain distance. We define the exchange energy as the difference of energies of Néel states  $|2\rangle$  and  $|1\rangle$  as  $E_{exch} = E_{\rightarrow\rightarrow} - E_{\rightarrow\leftarrow}$ , where  $\rightarrow\rightarrow$  and  $\rightarrow\leftarrow$  are determined by the mutual spin alignment of the Cr tip-apex (which is fixed) and the magnetic atom right underneath it ( $\rightarrow\rightarrow$  being parallel and  $\rightarrow\leftarrow$  antiparallel), as shown in Fig.1. When the tip is far away from the chain, or at the tunneling regime, the direct overlap between the  $d$  orbitals of the tip and magnetic atoms underneath is very weak, and the interaction between them can only be mediated by  $s$  and  $p$  electrons

§ As we know, the density functional theory employs periodic boundary conditions in calculations. However, we want to point out that in our calculations the spin states of AFM chains can also be tailored with a single tip, similar as that in experiments.<sup>2,11</sup>

of the atoms and the conduction electrons of the substrate. On a metal surface, where the density of conduction electrons is relatively high, this is known to lead to a ferromagnetic coupling of the  $d$ -shells of the adatoms via the Zener double-exchange mechanism.<sup>35,39–41</sup> In our case the decoupling influence of  $\text{Cu}_2\text{N}$  reduces the density of conduction electrons between the magnetic atoms and the substrate and thus the double exchange between the tip and the chain remains negligibly small. As the tip gets closer to the chain (at the contact regime) the direct exchange gains in magnitude, forcing the half-filled  $d$  shells to align antiferromagnetically, and the total energy difference of the system between two Néel states reaching values of several hundred meV.

The increase is especially pronounced for the Mn chain. Since the Cr atom and the Mn atom have similar ground state configurations, the two atoms have comparable density of states. Therefore, the hybridization between the Cr tip and the Mn atom is much stronger than in the case of Fe or Co chains. Still, even for Fe and Co chains, already at a distance of about 4–5 Å the exchange coupling becomes large enough to make one of the Néel states (in our sketch in Fig. 1(d) it is the state  $|1\rangle$ ) clearly preferable and lift the degeneracy into one of the classical ones.

Another important parameter of a magnetic system is its anisotropy. It defines the thermal stability of the system and the energy needed to switch the system from one spin state to the other. When 3 Fe atoms are adsorbed on  $\text{Cu}_2\text{N}/\text{Cu}(001)$  forming a finite chain, the distance between two Fe atoms is 7.2 Å.<sup>11</sup> As the tip positioned above the edge and the middle atom, the uniaxial magneto-crystalline anisotropy  $D$  is 2.1 meV and 3.6 meV, resulting in a magnetic anisotropy energy (MAE)  $DS^2$  of about 8.4 meV and 14.4 meV, respectively. The easy axis of the finite Fe chain is in-plane and along the chain.

For the compact Fe chain, we define the MAE of the chain as  $E_{\text{MAE}} = E_{\downarrow} - E_{\uparrow}$ , where  $E_{\downarrow}$  and  $E_{\uparrow}$  are the total energy of the system when the chain spins are aligned respectively along or perpendicular to the chain axis and the surface plane, which corresponds to the  $DS^2$  in experiments. Our calculations shown the value of the MAE to be 5.8 meV (or 1.45 meV/Fe atom), which is at the same order of the experiments.<sup>11</sup>

Let us consider how one could use the exchange interaction to tune the anisotropy of an AFM chain. The dependence of MAE on the distance between the tip and the chain is plotted in Fig. 2(a). Here, the spin direction of the tip is fixed to be out-of-plane which can be achieved in experiment<sup>8,42</sup>. At large tip-chain separations, or at the tunneling regime, the exchange interaction between the tip and the chain  $J_{ts}$  is calculated with  $J_{ts} = \Delta E / 2S_t S_s = (E_P - E_{AP}) / 2S_t S_s$ .  $\Delta E$  is the total energy difference of the system when the tip and the atom spins changes from parallel to antiparallel configuration. At the tunneling regime,  $J_{ts}$  is 0.67 meV, closely coincides with the experiments results.<sup>11</sup> The influence of the tip is again negligible and the Fe(Co) chain takes its lower-energy in-plane spin orientation while it is out-of-plane for the Mn chain.

The magnitude of the exchange interaction exponentially depends on the tip-chain distance. As the tip is brought closer, the coupling between the tip and the chain spins increases greatly and might become larger than the intrinsic crystalline anisotropy of the chain. Thus, the easy axis of the chain switches from in-plane

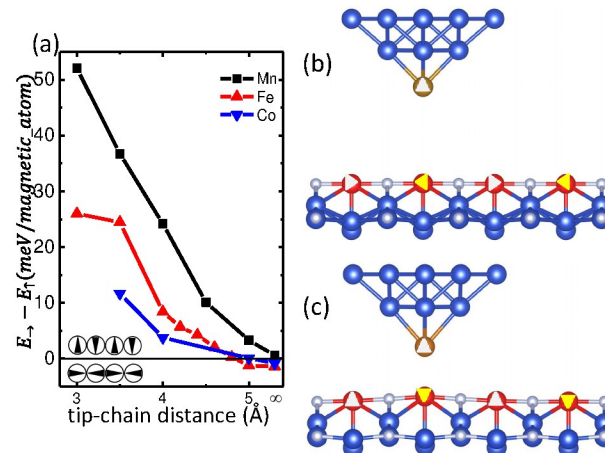


**Fig. 2** (a) Dependence of the magnetic anisotropy of AFM chains on  $\text{Cu}_2\text{N}/\text{Cu}(001)$  (defined as the total energy difference per magnetic atom between the chain states with spin aligned along and perpendicular to the axis of the chain) on the distance between the chain and a Cr-terminated tip with Cr spin fixed perpendicular to the surface. The last point marked with “ $\infty$ ” denotes the anisotropy of a chain in absence of a tip. (b) and (c) Schematic representation of the possible spin configurations with tip being far away (b) and close to the chains (c). Small triangles with different colors represent different spin directions.

to out-of-plane. For Fe chain, its spin orientation rotates from in-plane to out-of-plane at a tip-chain distance of about 4.8 Å. And the MAE of the Fe chain greatly increases by 20 times, reaching 26 meV/magnetic atom, at a tip-chain separation of 3 Å (at the contact regime). We thus see, that while AFM systems are not susceptible to conventional spin manipulation means like the external magnetic field, the MAE of such a system can be tuned by locally exchange-coupling it to a fixed magnetic entity like, for example, a spin-polarized STM tip.

As for our system, changes of the magnetic anisotropy is mainly due to the exchange coupling between the STM tip and the chain, not due to the SOC effect, although SOC with fully relativistic effect has been included in all calculations. This exchange interaction induced magnetic anisotropy can be qualitatively analyzed with the second-order perturbation formula<sup>43</sup>

$$\text{MAE} \sim \xi^2 \sum_{o,u} \frac{|\langle \psi_u | l_z | \psi_o \rangle|^2 - |\langle \psi_u | l_y | \psi_o \rangle|^2}{\epsilon_u - \epsilon_o}, \quad (1)$$

where the  $\xi$  parameter is an average of the spin orbital coupling coefficients,  $\{\psi_u, \psi_o\}$  stand for the unoccupied (occupied) states and  $\{l_y, l_z\}$  are the angular momentum operators, respectively.  $\epsilon_u$  and  $\epsilon_o$  are the energy levels of the unoccupied and occupied states. Obviously, to achieve a large MAE the system should show an increased states density near the Fermi level to enhance the numerator and have a narrow band to reduce the denominator in Eq. (1).

In the following part, we choose the Fe chain as a model system to analyze changes of the magnetic anisotropy of the system with Eq.(1). As the majority  $d$  states of Fe and Cr are fully occupied, changes of the MAE can only be attributed to the coupling between different  $d$  states in their minority parts. Therefore, we will focus on their minority states (Fig. 3). It can also be seen

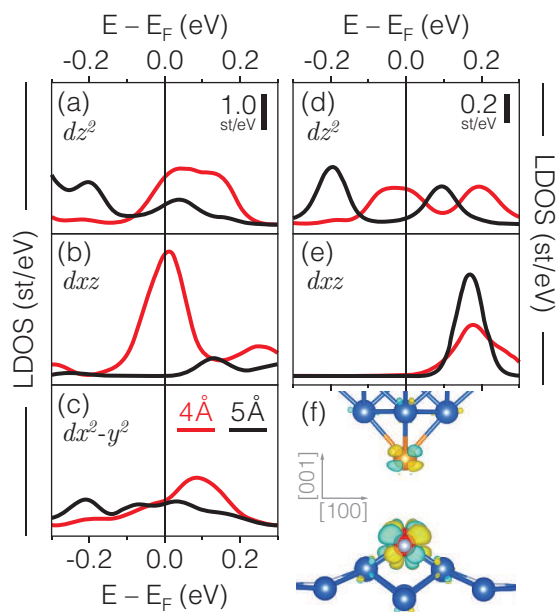


**Fig. 3** (a-c) PDOS of the Fe atom beneath the Cr tip at a tip chain distance of 5 Å and 4 Å. (d-e) PDOS of the Cr tip apex for the same configurations. (f) Iso-surfaces (iso-value of  $4 \cdot 10^{-4} \bar{e}/\text{\AA}^3$ ) of the spin density of the system at a tip chain distance of 4 Å. Yellow and blue represent positive and negative charge density difference.

from the spin density of the system, Fig. 3(f), that the magnetization of the chain and the tip mainly comes from the  $d_{xz}$  orbitals of the Fe atoms and  $d_{xz}$ ,  $d_{yz}$  orbitals of the Cr atom, respectively.

At a large tip-chain separation of 5 Å, the tip has a negligible effect on the chain due to weak interaction between them. Analyzing spin orbital coupling matrix elements, it can be found that the  $d_{z^2}$  orbital which couples with  $d_{xz}$  orbital through  $l_y$  operator  $\langle d_{z^2} | l_y | d_{xz} \rangle$  gives the largest contribution to the MAE through the second term in Eq. (1), which favors in-plane magnetization. It can also be seen from the left part of Fig. 3 that there are small peaks around the Fermi level in  $d_{z^2}$  and  $d_{x^2-y^2}$  orbital DOS. This explains the largest contribution to the MAE from  $\langle d_{z^2} | l_y | d_{xz} \rangle$  in the second term of Eq. (1). Therefore, at large tip-chain separations, the magnitude of MAE of the system is small, and the spin of the Fe chain prefers to lie in-plane of the surface.

At short tip-chain separations of about 4 Å, the exchange coupling between  $d_{xz}$  and  $d_{yz}$  through  $\langle d_{xz} | l_z | d_{yz} \rangle$  (out-of-plane) and that between  $d_{z^2}$  and  $d_{xz}$  through  $\langle d_{z^2} | l_y | d_{xz} \rangle$  (in-plane) gives vital contributions to the MAE through the first and the second terms in Eq. (1). Due to the strong direct interaction between the tip and the chain, the exchange coupling between the Cr tip-apex and the Fe chain should be taken into account. It can be seen from Fig. 3 (b) that near the Fermi level the strength of the  $d_{xz}$  orbital of Fe atoms is greatly increased and its band width is also greatly reduced. These results in a large enhancement of the first term in Eq. (1). Therefore, at short tip-chain separations, the magnetization of the Fe chain changes from in-plane to out-of-plane and the MAE magnitude of the system increases due to the strong coupling between the tip and the chain.

Further decreasing the tip-chain distance, the STM tip interacts

not only with the Fe atom just beneath it, but also with other Fe atoms in the chain, which will lead to an even larger increase in the magnitude of the MAE. Therefore, both of the sign and the magnitude of the MAE of an AFM Fe chain can be tuned with exchange coupling by varying the tip-chain distance.

Upon a closer look at Fig. 2 (a), it can be noticed that at short tip-chain distances, even at the same tip-chain separation, the MAE of the Mn chain is the biggest and that of the Co chain is the smallest, which can be attributed to the strong exchange coupling or hybridization between the Cr tip-apex and the Mn chain. Therefore, the exchange magnetic anisotropy is larger than that for the Fe(Co) chain.

According to the above analysis, it can be seen that the greatly increased magnetic anisotropy of the system at the contact regime is caused by the direct exchange coupling between  $d$  states of the tip and  $d$  states of the atom in the chain. With a spin polarized STM tip, we expect a great shift can be observed in the measured spin-excitation steps in IETS measurements as a function of tip height, especially at the contact regime. However, such phenomenon can not be observed with a non-magnetic tip<sup>11</sup>, which is mainly characterized by  $sp$  states.

### 3 Conclusions

In summary, we demonstrate that the exchange interaction can be used to manipulate magnetic properties of AFM materials. Our results reveal that the quantum ground state of an AFM material can be tuned into one of its Néel states by the exchange coupling with a spin polarized STM tip. Furthermore, the magnetic anisotropy of an AFM system can be tuned with the exchange coupling by varying the tip-substrate separation. The present work provides a theoretical prediction that it is feasible with current technology to manipulate magnetic properties of AFM materials.

### 4 Acknowledgement

The authors thank Oleg O. Brovko for stimulating discussions and his invaluable help in manuscript preparation. This work was supported by the National Natural Science Foundation of China (Grant No. NSFC-11274146), the National Basic Research Program of China (Grant No. 2012CB933101), the Fundamental Research Funds for the Central Universities (Grant No. 2022013zrc01), and the DFG through Collaborative Research Centre SFB 762 and through the dedicated project "Structure and magnetism of cluster ensembles on metal surfaces: microscopic theory of the fundamental interactions". PJ acknowledges support from the U.S. Department of Energy, Office of Basic Energy Sciences, Division of Materials Sciences and Engineering under award DE-FG02-96ER45579.

### References

- 1 D. Ralph and M. Stiles, *J. Magn. Magn. Mater.*, 2008, **320**, 1190 – 1216.
- 2 S. Loth, S. Baumann, C. P. Lutz, D. M. Eigler and A. J. Heinrich, *Science*, 2012, **335**, 196–199.
- 3 B. G. Park, J. Wunderlich, X. Martí, V. Holý, Y. Kurosaki, M. Yamada, H. Yamamoto, A. Nishide, J. Hayakawa, H. Takahashi, A. B. Shick and T. Jungwirth, *Nat Mater*, 2011, **10**, 347–351.

- 4 Y. Y. Wang, C. Song, B. Cui, G. Y. Wang, F. Zeng and F. Pan, *Phys. Rev. Lett.*, 2012, **109**, 137201.
- 5 X. Marti, I. Fina, C. Frontera, J. Liu, P. Wadley, Q. He, R. J. Paull, J. D. Clarkson, J. Kudrnovsk, I. Turek, J. Kune, D. Yi, J.-H. Chu, C. T. Nelson, L. You, E. Arenholz, S. Salahuddin, J. Fontcuberta, T. Jungwirth and R. Ramesh, *Nat Mater*, 2014, **13**, 367–374.
- 6 C. F. Hirjibehedin, C. P. Lutz and A. J. Heinrich, *Science*, 2006, **312**, 1021–1024.
- 7 P. Wahl, P. Simon, L. Diekhöner, V. S. Stepanyuk, P. Bruno, M. A. Schneider and K. Kern, *Phys. Rev. Lett.*, 2007, **98**, 056601.
- 8 L. Zhou, J. Wiebe, S. Lounis, E. Vedmedenko, F. Meier, S. Blugel, P. H. Dederichs and R. Wiesendanger, *Nat Phys*, 2010, **6**, 187–191.
- 9 A. A. Khajetoorians, J. Wiebe, B. Chilian and R. Wiesendanger, *Science*, 2011, **332**, 1062–1064.
- 10 J.-P. Gauyacq, S. M. Yaro, X. Cartoixà and N. Lorente, *Phys. Rev. Lett.*, 2013, **110**, 087201.
- 11 S. Yan, D.-J. Choi, B. A. J., S. Rolf-Pissarczyk and S. Loth, *Nat Nano*, 2014, **10**, 40–45.
- 12 J. Dorantes-Dávila, H. Dreyssé and G. M. Pastor, *Phys. Rev. Lett.*, 2003, **91**, 197206.
- 13 G. Moulas, A. Lehnert, S. Rusponi, J. Zabloudil, C. Etz, S. Ouazi, M. Etzkorn, P. Bencok, P. Gambardella, P. Weinberger and H. Brune, *Phys. Rev. B*, 2008, **78**, 214424.
- 14 A. Lehnert, S. Dennler, P. Błoński, S. Rusponi, M. Etzkorn, G. Moulas, P. Bencok, P. Gambardella, H. Brune and J. Hafner, *Phys. Rev. B*, 2010, **82**, 094409.
- 15 M. Weisheit, S. Fähler, A. Marty, Y. Souche, C. Poinignon and D. Givord, *Science*, 2007, **315**, 349–351.
- 16 C.-G. Duan, J. P. Velev, R. F. Sabirianov, Z. Zhu, J. Chu, S. S. Jaswal and E. Y. Tsybal, *Phys. Rev. Lett.*, 2008, **101**, 137201.
- 17 J. Hu and R. Wu, *Phys. Rev. Lett.*, 2013, **110**, 097202.
- 18 T. R. Dasa, P. Ruiz-Díaz, O. O. Brovko and V. S. Stepanyuk, *Phys. Rev. B*, 2013, **88**, 104409.
- 19 A. Sonntag, J. Hermenau, A. Schlenhoff, J. Friedlein, S. Krause and R. Wiesendanger, *Phys. Rev. Lett.*, 2014, **112**, 017204.
- 20 O. O. Brovko, P. Ruiz-Daz, T. R. Dasa and V. S. Stepanyuk, *J. Phys: Condens. Matter*, 2014, **26**, 093001.
- 21 B. Bryant, A. Spinelli, J. J. T. Wagenaar, M. Gerrits and A. F. Otte, *Phys. Rev. Lett.*, 2013, **111**, 127203.
- 22 J. C. Oberg, M. R. Calvo, F. Delgado, M. Moro-Lagares, D. Serate, D. Jacob, J. Fernandez-Rossier and C. F. Hirjibehedin, *Nat Nano*, 2013, **9**, 64–68.
- 23 P. Ruiz-Díaz, T. R. Dasa and V. S. Stepanyuk, *Phys. Rev. Lett.*, 2013, **110**, 267203.
- 24 P. Gambardella, S. Rusponi, M. Veronese, S. S. Dhesi, C. Grazioli, A. Dallmeyer, I. Cabria, R. Zeller, P. H. Dederichs, K. Kern, C. Carbone and H. Brune, *Science*, 2003, **300**, 1130–1133.
- 25 C. F. Hirjibehedin, C.-Y. Lin, A. F. Otte, M. Ternes, C. P. Lutz, B. A. Jones and A. J. Heinrich, *Science*, 2007, **317**, 1199–1203.
- 26 I. G. Rau, S. Baumann, S. Rusponi, F. Donati, S. Stepanow, L. Gragnaniello, J. Dreiser, C. Piamonteze, F. Nolting, S. Gangopadhyay, O. R. Albertini, R. M. Macfarlane, C. P. Lutz, B. A. Jones, P. Gambardella, A. J. Heinrich and H. Brune, *Science*, 2014, **344**, 988–992.
- 27 P. Gambardella, *Nat Mater*, 2006, **5**, 431–432.
- 28 H. Brune, *Science*, 2006, **312**, 1005–1006.
- 29 D. Das, H. Singh, T. Chakraborty, R. K. Gopal and C. Mitra, *New J. Phys*, 2013, **15**, 013047.
- 30 S. Holzberger, T. Schuh, S. Blügel, S. Lounis and W. Wulfhchel, *Phys. Rev. Lett.*, 2013, **110**, 157206.
- 31 G. Kresse and J. Hafner, *Phys. Rev. B*, 1993, **47**, 558–561.
- 32 G. Kresse and J. Furthmüller, *Phys. Rev. B*, 1996, **54**, 11169–11186.
- 33 P. E. Blöchl, *Phys. Rev. B*, 1994, **50**, 17953–17979.
- 34 J. P. Perdew, K. Burke and M. Ernzerhof, *Phys. Rev. Lett.*, 1996, **77**, 3865–3868.
- 35 K. Tao, V. S. Stepanyuk, W. Hergert, I. Rungger, S. Sanvito and P. Bruno, *Phys. Rev. Lett.*, 2009, **103**, 057202.
- 36 A. B. Shick, F. Mácá and A. I. Lichtenstein, *Phys. Rev. B*, 2009, **79**, 172409.
- 37 C.-Y. Lin and B. A. Jones, *Phys. Rev. B*, 2011, **83**, 014413.
- 38 J. W. Nicklas, A. Wadehra and J. W. Wilkins, *J. Appl. Phys.*, 2011, **110**, 123915.
- 39 C. Zener, *Phys. Rev.*, 1951, **82**, 403–405.
- 40 C. Zener, *Phys. Rev.*, 1951, **81**, 440–444.
- 41 R. Schmidt, C. Lazo, U. Kaiser, A. Schwarz, S. Heinze and R. Wiesendanger, *Phys. Rev. Lett.*, 2011, **106**, 257202.
- 42 A. Schlenhoff, S. Krause, G. Herzog and R. Wiesendanger, *Appl. Phys. Lett.*, 2010, **97**, 083104.
- 43 D.-s. Wang, R. Wu and A. J. Freeman, *Phys. Rev. B*, 1993, **47**, 14932–14947.